Science Advances
AAAS

Supplementary Materials for

Gas-phase synthesis of anthracene and phenanthrene via radical-radical reaction induced ring expansions

Shane J. Goettl *et al.*

Corresponding author: Patrick Hemberger, patrick.hemberger@psi.ch; Alexander M. Mebel, mebela@fiu.edu; Ralf I. Kaiser, ralfk@hawaii.edu

Sci. Adv. **11**, eadv0692 (2025)
DOI: 10.1126/sciadv.adv0692

The PDF file includes:

Other Supplementary Material for this manuscript includes the following:

Supplementary Text

Possible formation pathways of the $C_{14}H_{10}$ isomers (*trans*-1-vinylacenaphthylene, *cis*-1-vinylacenaphthylene, 1-/3-fulvenyl[*a*]naphthalene, and 1-fulvenyl[*b*]naphthalene) which feature simulated Franck-Condon spectra (Fig. S5) that may contribute to the 7.6–7.8 eV region of the experimental ms-TPES (Fig. 2) are detailed here. All five isomers require hydrogen-atom-assisted isomerization of phenanthrene, with the pathways to *trans*- and *cis*-1-vinylacenaphthylene shown in Fig. 4. First, a hydrogen atom adds to the C4 carbon of phenanthrene (**p1** → **i16**), followed by opening of the six-membered ring (**i16** → **i17**), a series of bond rotations and hydrogen atom migrations (**i17** → **i18** → **i19** → **i20** → **i21**), four-membered ring closure (**i21** → **i23**) and opening (**i23** → **i24**) on the naphthyl moiety, two hydrogen atom shifts (**i24** → **i25** → **i26**), migration of the side chain from the 2- to the 1-position of the naphthyl group (**i26** → **i27**), hydrogen atom shift from the side chain to the ring (**i27** → **i28**), five-membered ring closure in the three-carbon bay of the naphthyl moiety (**i28** → **i29**), and finally atomic hydrogen loss to *trans*- and *cis*-1-vinylacenaphthylene (**i29** → **p7**/**p7′**). Pathways to the fulvenylnaphthalene isomers may commence from different points on the route to **p7**/**p7′**. Specifically, **i18** and/or **i19** may undergo five-membered ring closure and atomic hydrogen loss to form 1-fulvenyl[*a*]naphthalene, while the same mechanism can lead from **i20** and **i21** to 1-fulvenyl[*b*]naphthalene. A rotation of the side chain of **i28** followed by five-membered ring closure and hydrogen atom ejection may lead to 3-fulvenyl[*a*]naphthalene. Additional pathways open up if the hydrogen-atom-assisted isomerization of phenanthrene is initialized from the C1 carbon, which will cause the six-membered ring to open up from the opposite side. In this case, the intermediates equivalent to **i18** and **i19** would instead lead to 3-fulvenyl[*a*]naphthalene after five-membered ring closure and hydrogen atom loss. While this list of reaction routes is not exhaustive, it shows the feasibility of forming the mentioned $C_{14}H_{10}$ isomers from the title reaction.

Outline of Reaction Kinetics

Accurate theoretical prediction of the phenanthrene to anthracene branching ratio represents an extremely computationally demanding task because the critical determining factor is the branching in the entrance channel between **i1** and **i6**, which could be, in principle, evaluated employing the variable reaction coordinate transition state theory (VRC-TST) – the calculations requiring energy assessments for tens of thousands of structures of fluorenyl and methyl reactants approaching each other. The channel via **i1** depending on temperature and pressure can either produce the thermalized **i1** complex or **i2** + H, through the well-skipping channel (see Table S1). The **i2** + H pair can also form by thermal unimolecular decomposition of **i1** in a secondary reaction. Once **i2** is produced, it undergoes rapid dissociation to either dibenzofulvene (**p3**) + H (93%) or phenanthrene (**p1**) + H (7%) with its lifetime being on a submicrosecond scale. Next, **p3** can undergo H-assisted isomerization to **p1** with a bimolecular rate constant of $\sim 2\times10^{-11}$ cm^3 molecule^{-1} s^{-1} at the experimental temperature and pressure. The rate constants presented in Table S1 were computed using the Rice-Ramsperger-Kassel-Marcus Master Equation approach (RRKM-ME) (*87*) in conjunction with phase space theory (*88*) for the barrierless entrance and exit channels of the primary reaction on the singlet surface using the MESS package (*89*). The triplet surface is not expected to contribute to the overall reaction significantly, because of the strongly repulsive character of the potential (Fig. S6C).

Alternatively, the channel via **i6** can either produce thermalized **i6** or **i7** + H, where **i7** is not stable at high temperatures and would instantly dissociate to anthracene (**p2**) + H practically exclusively. The H-assisted isomerization of phenanthrene to other $C_{14}H_{10}$ isomers including anthracene and the corresponding reverse reactions (Fig. 4) also need to be included in the complex kinetic mechanism. This complexity of the kinetics of the investigated system alleviated by the necessity of computation fluid dynamics modeling of the gas flow in the reactor where the temperature, pressure and the gas velocity vary make the branching ratio calculations a challenging task which can be addressed in a future work.

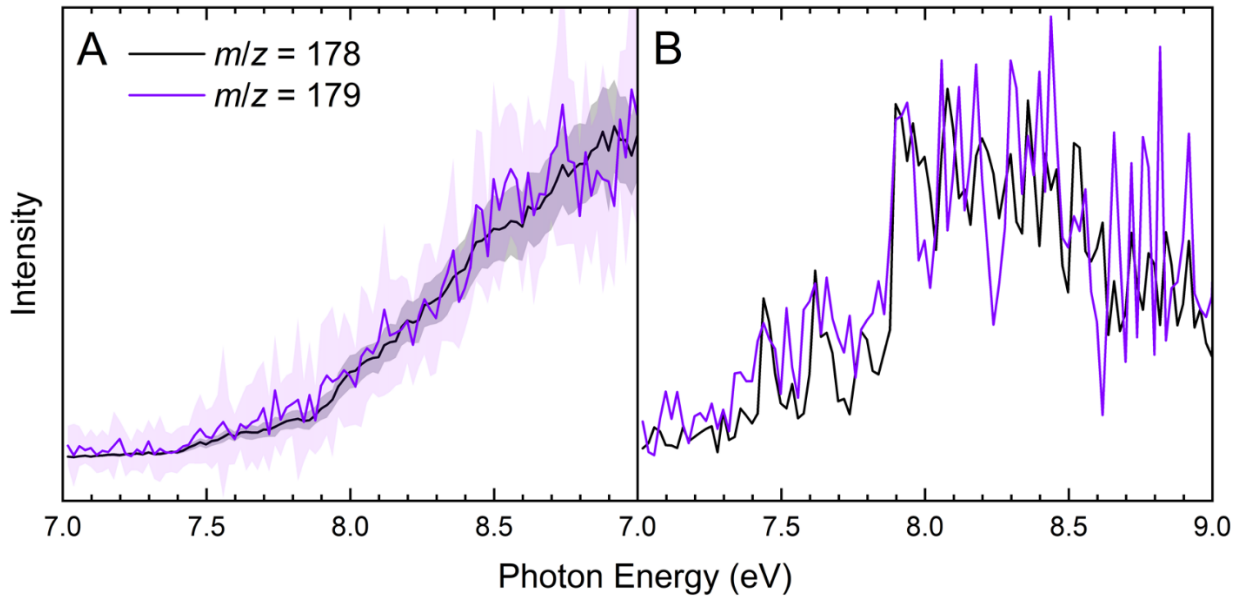

Fig. S1. Experimental spectra at m/z = 178 and 179. Photoionization efficiency (PIE) curves (**A**) and mass-selective threshold photoelectron (ms-TPE) spectra (**B**) for the acetone (C_3H_6O) – 9-bromofluorene ($C_{13}H_9Br$) system taken at *m*/*z* = 178 (black) and 179 (violet) at a reactor temperature of 1700 ± 100 K. The overall error bars (gray and faded violet areas) consist of two parts: 1 σ error of the PIE curve averaged over the individual scans and ±10% based on the accuracy of the photodiode.

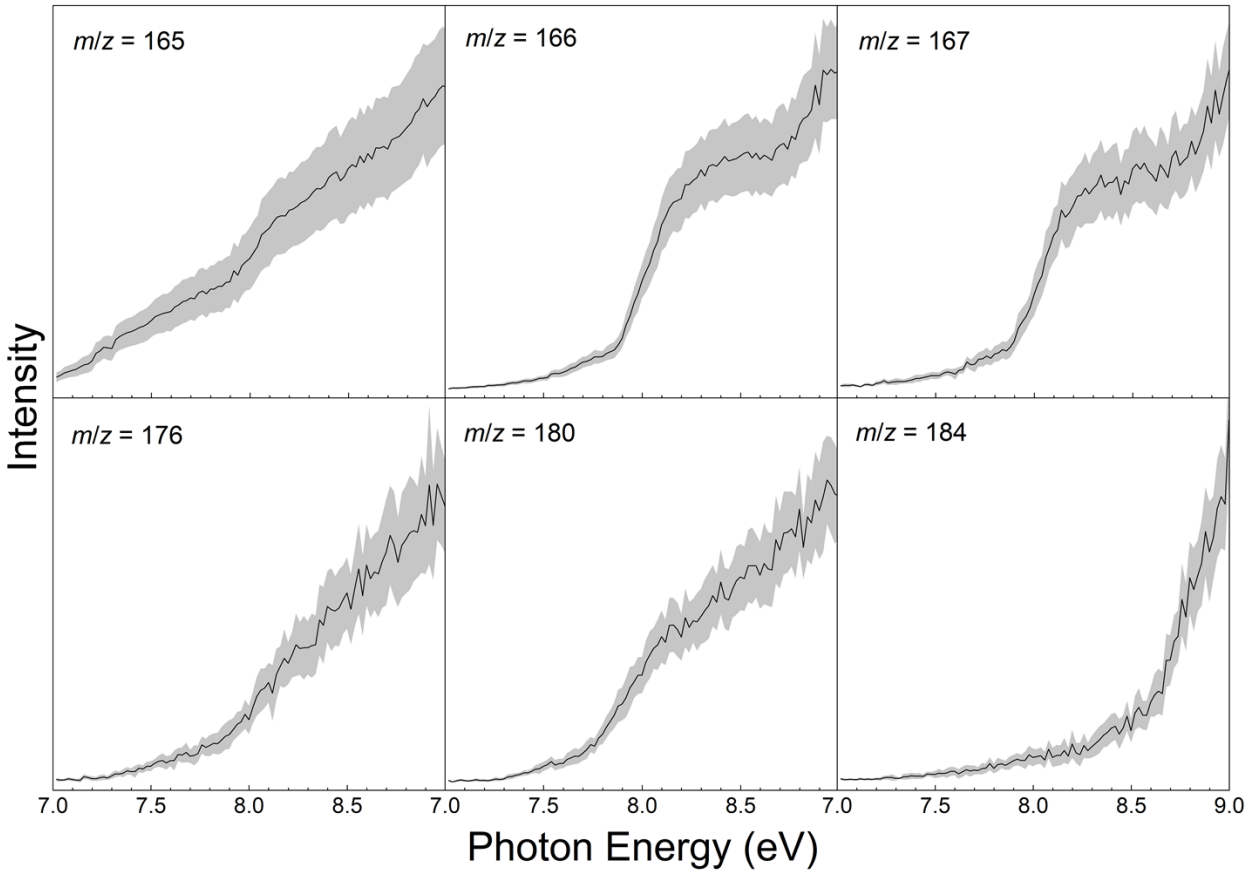

Fig. S2. Photoionization efficiency (PIE) curves of other masses. PIE curves of other products (*m*/*z* = 165–184) for the acetone (C_3H_6O) – 9-bromofluorene ($C_{13}H_9Br$) system at a reactor temperature of 1700 ± 100 K. The overall error bars (gray area) consist of two parts: 1 σ error of the PIE curve averaged over the individual scans and ±10% based on the accuracy of the photodiode.

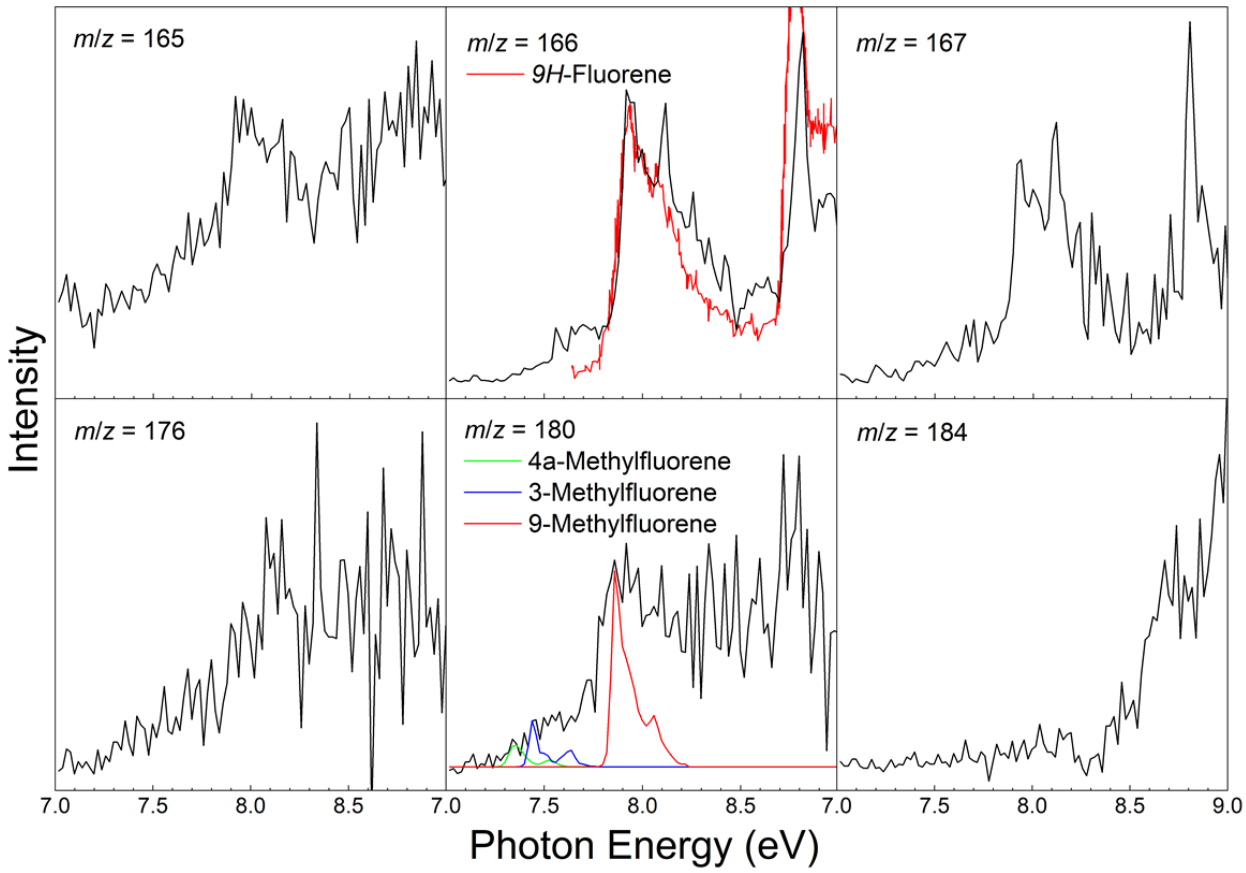

Fig. S3. Mass-selected threshold photoelectron (ms-TPE) spectra of other masses. ms-TPE spectra of other products (m/z = 165–184) for the acetone (C_3H_6O) – 9-bromofluorene ($C_{13}H_9Br$) system at a reactor temperature of 1700 ± 100 K. The reference photoelectron spectrum of *9H*-fluorene digitized from Maier and Turner (*90*) is shown at m/z = 166, and calculated spectra for methylfluorene isomers are shown at m/z = 180.

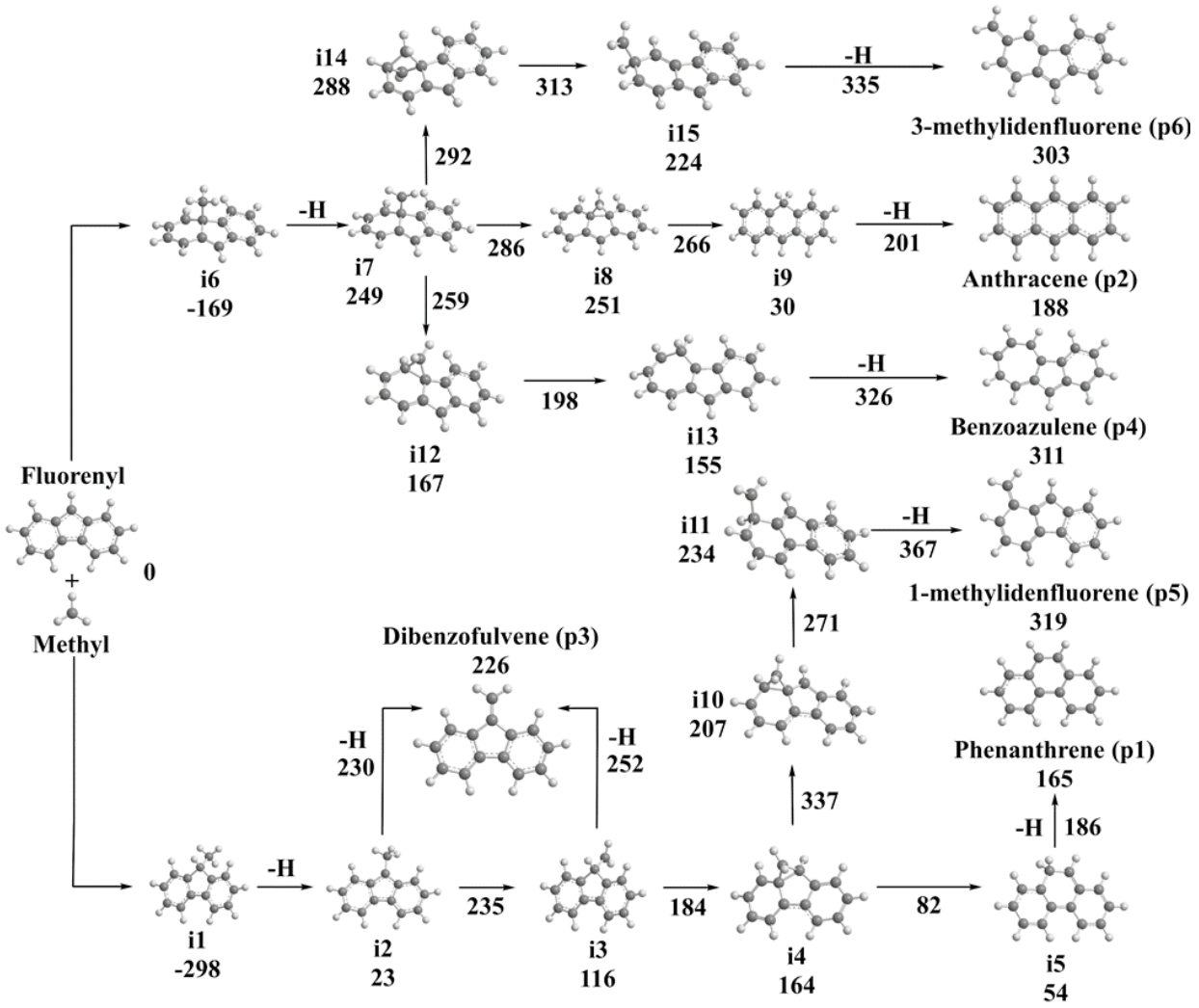

Fig. S4. Addition pathways of the potential energy diagram. Schematic potential energy diagram for the reaction of the methyl radical (CH_3) with the fluorenyl radical ($C_{13}H_9$) calculated at the G3(MP2,CC)//ωB97XD/6-311G(d,p) level of theory showing additional pathways. Energies are in kJ mol^{-1}.

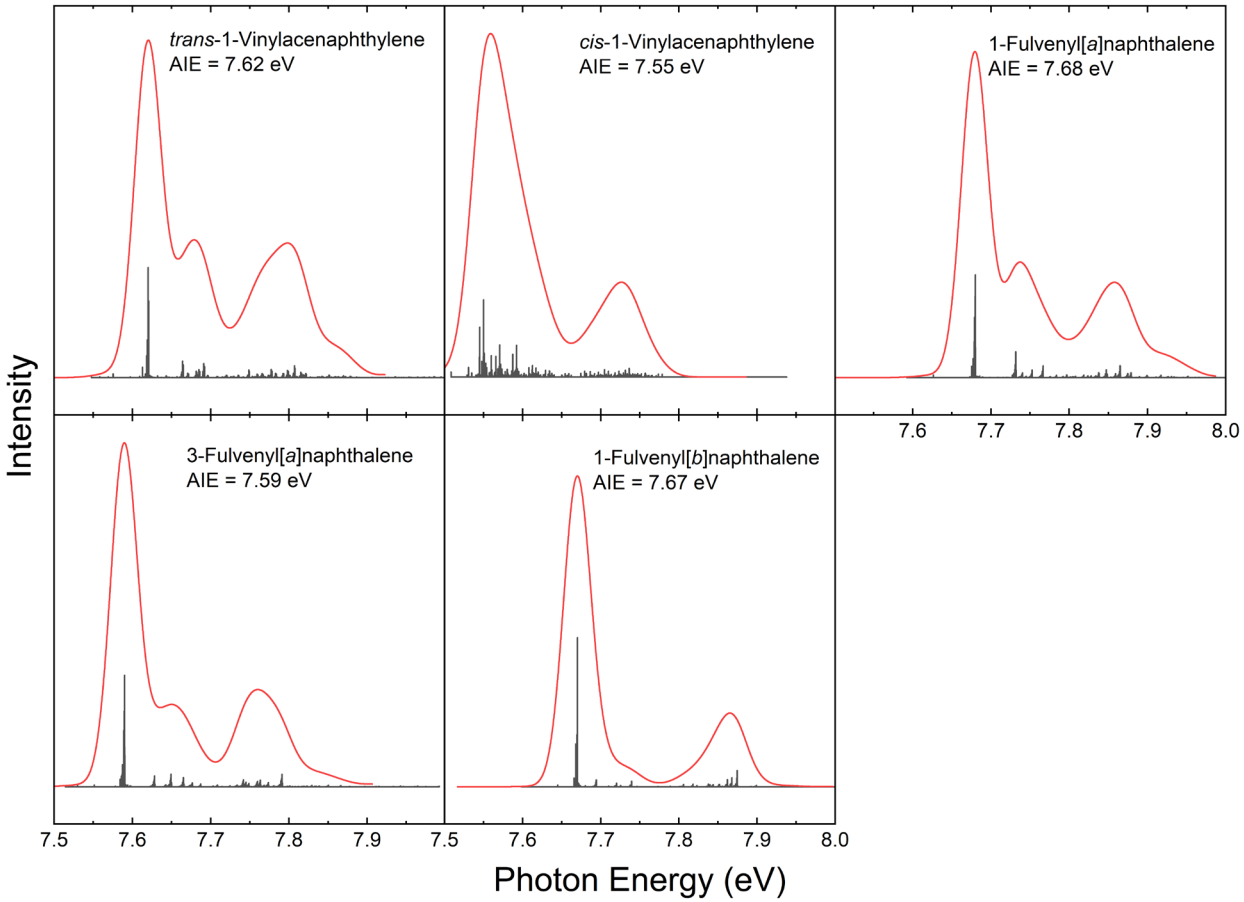

Fig. S5. Simulated spectra of additional isomers. FC stick spectra and Gaussian convoluted spectra of the five $C_{14}H_{10}$ isomers *trans*-1-vinylacenaphthylene, *cis*-1-vinylacenaphthylene, 1-fulvenyl[*a*]naphthalene, 3-fulvenyl[*a*]naphthalene, and 1-fulvenyl[*b*]naphthalene.

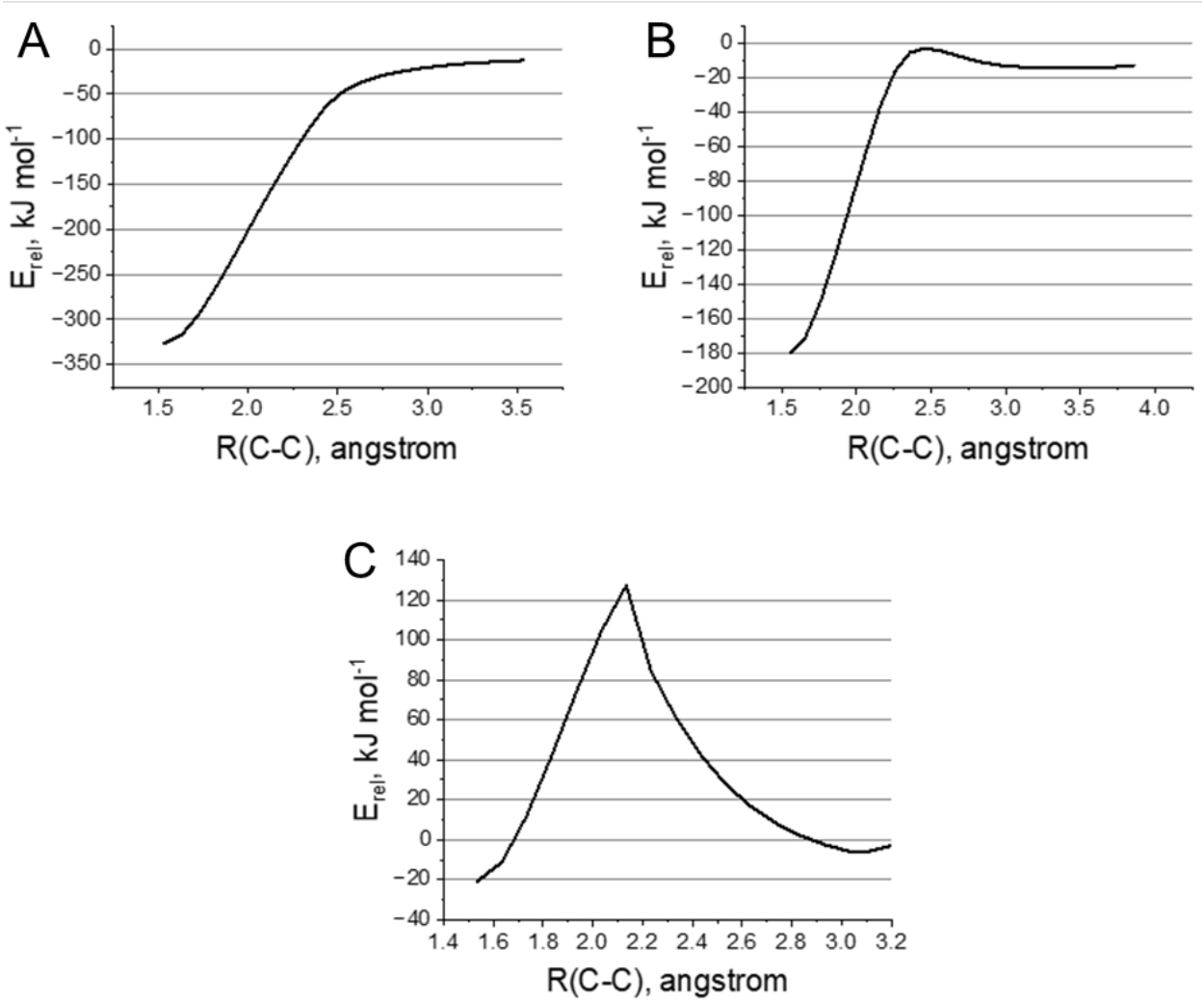

Fig. S6. Entrance channel minimal energy paths (MEPs). MEP potential energy profiles for the entrance channels of the $CH_3^{\bullet}$ + $C_{13}H_9^{\bullet}$ reaction leading to singlet i1 (A), singlet i6 (B), and triplet i1 (C). The MEPs were explored at the unrestricted DFT level, UωB97XD/6-311G(d,p). Unrestricted DFT calculations have been demonstrated to portray the potential and geometric structures on pathways of recombination of two radicals adequately, at least qualitatively (*91, 92*). While both (A) and (B) show the absence of barriers above the energy level of separated reactants, the MEP toward i6 on the singlet surface (B) is less attractive than toward i1 (A) and hints at existence of a van der Waals (vdW) complex and a submerged transition state. However, neither of such stationary points on the path could be actually located upon full geometry optimization. Alternatively, the triplet potential energy profile is slightly attractive at long separations and a vdW complex of fluorenyl and CH_3 can be formed in the triplet state. As the two radicals approach one another, the energy sharply increases and goes over a maximum at ~127 kJ mol^{-1}. This illustrates that the triplet channel is not competitive with either addition on the singlet surface. The triplet channel might contribute to the overall reaction rate only at low temperatures when the vdW complex can survive long enough to undergo intersystem crossing to the singlet state in case spin-orbit coupling is sufficiently strong. Based on this, we conclude that the triplet surface is not relevant to the conditions of the present experiment.

Table S1. **Rate constants.** Calculated rate constants for most important reaction channels.

(a) Bimolecular $CH_3^\bullet + C_{13}H_9^\bullet \rightarrow C_{14}H_{12}$(**i1**) reaction ($cm^3$ $molecule^{-1}$ s^{-1}) and unimolecular decomposition of **i1** (s^{-1}).

	0.03 atm			1 atm		
T(K)	$CH_3^\bullet + C_{13}H_9^\bullet \rightarrow$ **i1**	$CH_3^\bullet + C_{13}H_9^\bullet \rightarrow$ **i2**+H	**i1**→**i2**+H	$CH_3^\bullet + C_{13}H_9^\bullet \rightarrow$ **i1**	$CH_3^\bullet + C_{13}H_9^\bullet \rightarrow$ **i2**+H	**i1**→**i2**+H
500	3.99E-11	1.34E-21	9.66E-19	3.99E-11	4.02E-23	9.66E-19
600	3.18E-11	4.54E-20	4.68E-13	3.18E-11	1.36E-21	4.68E-13
700	2.55E-11	7.33E-19	5.07E-09	2.55E-11	2.20E-20	5.07E-09
800	2.02E-11	6.96E-18	4.98E-06	2.02E-11	2.09E-19	4.98E-06
900	1.56E-11	4.48E-17	9.68E-04	1.56E-11	1.34E-18	9.68E-04
1000	1.17E-11	2.15E-16	6.02E-02	1.17E-11	6.46E-18	6.02E-02
1125	7.86E-12	1.11E-15	3.33E+00	7.90E-12	3.36E-17	3.36E+00
1250	5.06E-12	4.17E-15	7.29E+01	5.18E-12	1.29E-16	7.50E+01
1375	3.07E-12	1.14E-14	7.89E+02	3.32E-12	3.72E-16	8.63E+02
1500	1.71E-12	2.30E-14	4.84E+03	2.11E-12	8.30E-16	6.06E+03
1650	7.18E-13	3.77E-14	2.28E+04	1.20E-12	1.65E-15	3.85E+04
1750	3.52E-13	4.35E-14	4.65E+04	8.25E-13	2.31E-15	1.04E+05
1800	2.37E-13	4.45E-14	6.14E+04	6.82E-13	2.65E-15	1.62E+05
2000		4.18E-14		3.16E-13	4.10E-15	6.87E+05
2250		2.42E-14		1.12E-13	6.19E-15	2.31E+06
2500		1.40E-14			1.40E-14	

(b) Unimolecular decomposition of $C_{14}H_{11}$(**i2**) (s^{-1}) and H-assisted isomerization of dibenzofulvene (**p3**) to phenanthrene (**p1**) reaction (cm^3 $molecule^{-1}$ s^{-1}).

	0.03 atm			1 atm		
T(K)	**i2**→**p1**+H	**i2**→**p3**+H	**p3**+H→**p1**+H	**i2**→**p1**+H	**i2**→**p3**+H	**p3**+H→**p1**+H
500	1.17E-12	7.77E-09	1.52E-16	4.68E-15	7.77E-09	7.42E-19
600	6.89E-08	4.46E-05	4.12E-15	6.47E-10	4.46E-05	4.70E-17
700	1.88E-04	2.27E-02	4.58E-14	4.16E-06	2.27E-02	1.21E-15
800	6.35E-02	2.50E+00	2.57E-13	3.19E-03	2.51E+00	1.49E-14
900	4.59E+00	9.70E+01	8.92E-13	5.22E-01	1.00E+02	1.01E-13
1000	1.06E+02	1.70E+03	2.31E-12	2.58E+01	1.93E+03	4.26E-13
1125	1.67E+03	2.39E+04	5.64E-12	1.10E+03	3.64E+04	1.63E-12
1250	1.15E+04	1.45E+05	1.01E-11	1.44E+04	3.44E+05	4.18E-12
1375	3.78E+04	4.87E+05	1.40E-11	8.49E+04	1.81E+06	8.08E-12
1500			1.78E-11	4.16E+05	5.99E+06	1.31E-11
1650			1.98E-11	1.12E+06	1.65E+07	1.73E-11
1750			2.10E-11			2.10E-11
1800			2.15E-11			2.15E-11
2000			2.31E-11			2.31E-11
2250			2.43E-11			2.43E-11
2500			2.49E-11			2.49E-11

Data S1. Calculated parameters of all species. Optimized Cartesian coordinates (Å) and vibrational frequencies (cm^{-1}) for all intermediates, transition states, reactants, and products involved in the $C_{13}H_9$ + CH_3 reaction at the G3(MP2,CC)//ωB97XD/6-311G** level.

REFERENCES AND NOTES

1. I. Ratera, J. Veciana, Playing with organic radicals as building blocks for functional molecular materials. *Chem. Soc. Rev.* **41**, 303–349 (2012).

2. S. Sanvito, Molecular spintronics. *Chem. Soc. Rev.* **40**, 3336–3355 (2011).

3. T. Janoschka, M. D. Hager, U. S. Schubert, Powering up the future: Radical polymers for battery applications. *Adv. Mater.* **24**, 6397–6409 (2012).

4. D. Yuan, Y. Guo, Y. Zeng, Q. Fan, J. Wang, Y. Yi, X. Zhu, Air-stable n-type thermoelectric materials enabled by organic diradicaloids. *Angew. Chem. Int. Ed.* **58**, 4958–4962 (2019).

5. T. Minami, M. Nakano, Diradical character view of singlet fission. *J. Phys. Chem. Lett.* **3**, 145–150 (2012).

6. Q. Peng, A. Obolda, M. Zhang, F. Li, Organic light-emitting diodes using a neutral π radical as emitter: The emission from a doublet. *Angew. Chem. Int. Ed.* **54**, 7091–7095 (2015).

7. M. Agúndez, C. Cabezas, B. Tercero, N. Marcelino, J. D. Gallego, P. de Vicente, J. Cernicharo, Discovery of the propargyl radical (CH_2CCH) in TMC-1: One of the most abundant radicals ever found and a key species for cyclization to benzene in cold dark clouds. *Astron. Astrophys.* **647**, L10 (2021).

8. M. Agúndez, N. Marcelino, C. Cabezas, R. Fuentetaja, B. Tercero, P. de Vicente, J. Cernicharo, Detection of the propargyl radical at λ 3 mm. *Astron. Astrophys.* **657**, A96 (2022).

9. C. Cabezas, M. Agúndez, N. Marcelino, B. Tercero, J. R. Pardo, P. de Vicente, J. Cernicharo, Discovery of interstellar 3-cyano propargyl radical, CH_2CCCN. *Astron. Astrophys.* **654**, L9 (2021).

10. P. Thaddeus, C. Gottlieb, A. Hjalmarson, L. Johansson, W. Irvine, P. Friberg, R. Linke, Astronomical identification of the C_3H radical. *Astrophys. J.* **294**, L49 (1985).

11. J. Cernicharo, C. Kahane, J. Gomez-Gonzalez, M. Guélin, Tentative detection of the C_5H radical. *Astron. Astrophys.* **164**, L1 (1986).

12. W. M. Irvine, P. Friberg, A. Hjalmarson, S. Ishikawa, N. Kaifu, K. Kawaguchi, S. Madden, H. Matthews, M. Ohishi, S. Saito, H. Suzuki, P. Thaddeus, B. E. Turner, S. Yamamoto, L. M. Ziurys, Identification of the interstellar cyanomethyl radical (CH_2CN) in the molecular clouds TMC-1 and Sagittarius B2. *Astrophys. J.* **334**, L107 (1988).

13. J. Cernicharo, M. Guélin, J. R. Pardo, Detection of the linear radical HC_4N in IRC +10216. *Astrophys. J.* **615**, L145–L148 (2004).

14. J. Cernicharo, M. Agúndez, C. Cabezas, B. Tercero, N. Marcelino, R. Fuentetaja, J. R. Pardo, P. de Vicente, Discovery of HCCCO and C_5O in TMC-1 with the QUIJOTE line survey. *Astron. Astrophys.* **656**, L21 (2021).

15. K. O. Johansson, M. P. Head-Gordon, P. E. Schrader, K. R. Wilson, H. A. Michelsen, Resonance-stabilized hydrocarbon-radical chain reactions may explain soot inception and growth. *Science* **361**, 997–1000 (2018).

16. S. Sinha, R. K. Rahman, A. Raj, On the role of resonantly stabilized radicals in polycyclic aromatic hydrocarbon (PAH) formation: Pyrene and fluoranthene formation from benzyl–Indenyl addition. *Phys. Chem. Chem. Phys.* **19**, 19262–19278 (2017).

17. D. E. Couch, A. J. Zhang, C. A. Taatjes, N. Hansen, Experimental observation of hydrocarbon growth by resonance-stabilized radical–Radical chain reaction. *Angew. Chem. Int. Ed.* **60**, 27230–27235 (2021).

18. J. A. Rundel, C. M. Thomas, P. E. Schrader, K. R. Wilson, K. O. Johansson, R. P. Bambha, H. A. Michelsen, Promotion of particle formation by resonance-stabilized radicals during hydrocarbon pyrolysis. *Combust. Flame* **243**, 111942 (2022).

19. C. Y. Wang, L. Zhao, R. I. Kaiser, Gas-phase preparation of the 14π Hückel polycyclic aromatic anthracene and phenanthrene isomers ($C_{14}H_{10}$) via the Propargyl Addition–BenzAnnulation (PABA) mechanism. *ChemPhysChem* **25**, e202400151 (2024).

20. A. G. G. M. Tielens, Interstellar polycyclic aromatic hydrocarbon molecules. *Annu. Rev. Astron. Astrophys.* **46**, 289–337 (2008).

21. B. A. McGuire, R. A. Loomis, A. M. Burkhardt, K. L. K. Lee, C. N. Shingledecker, S. B. Charnley, I. R. Cooke, M. A. Cordiner, E. Herbst, S. Kalenskii, M. A. Siebert, E. R. Willis, C. Xue, A. J. Remijan, M. C. McCarthy, Detection of two interstellar polycyclic aromatic hydrocarbons via spectral matched filtering. *Science* **371**, 1265–1269 (2021).

22. M. L. Sita, P. B. Changala, C. Xue, A. M. Burkhardt, C. N. Shingledecker, K. L. K. Lee, R. A. Loomis, E. Momjian, M. A. Siebert, D. Gupta, E. Herbst, A. J. Remijan, M. C. McCarthy, I. R. Cooke, B. A. McGuire, Discovery of interstellar 2-cyanoindene (2-C_9H_7CN) in GOTHAM observations of TMC-1. *Astrophys. J. Lett.* **938**, L12 (2022).

23. D. Loru, C. Cabezas, J. Cernicharo, M. Schnell, A. L. Steber, Detection of ethynylbenzene in TMC-1 and the interstellar search for 1,2-diethynylbenzene. *Astron. Astrophys.* **677**, A166 (2023).

24. L. Becker, T. E. Bunch, Fullerenes, fulleranes and polycyclic aromatic hydrocarbons in the Allende meteorite. *Meteorit. Planet. Sci.* **32**, 479–487 (1997).

25. B. P. Basile, B. S. Middleditch, J. Oró, Polycyclic aromatic hydrocarbons in the Murchison meteorite. *Org. Geochem.* **5**, 211–216 (1984).

26. T. J. Wdowiak, G. C. Flickinger, J. R. Cronin, Insoluble organic material of the Orgueil carbonaceous chondrite and the unidentified infrared bands. *Astrophys. J.* **328**, L75–L79 (1988).

27. S. S. Zeichner, J. C. Aponte, S. Bhattacharjee, G. Dong, A. E. Hofmann, J. P. Dworkin, D. P. Glavin, J. E. Elsila, H. V. Graham, H. Naraoka, Y. Takano, S. Tachibana, A. T. Karp, K. Grice, A. I. Holman, K. H. Freeman, H. Yurimoto, T. Nakamura, T. Noguchi, R. Okazaki, H. Yabuta, K. Sakamoto, T. Yada, M. Nishimura, A. Nakato, A. Miyazaki, K. Yogata, M. Abe, T. Okada, T. Usui, M. Yoshikawa, T. Saiki, S. Tanaka, F. Terui, S. Nakazawa, S.-i. Watanabe, Y. Tsuda, K. Hamase, K. Fukushima, D. Aoki, M. Hashiguchi, H. Mita, Y. Chikaraishi, N. Ohkouchi, N. O. Ogawa, S. Sakai, E. T. Parker, H. L. McLain, F.-R. Orthous-Daunay, V. Vuitton, C. Wolters, P. Schmitt-Kopplin, N. Hertkorn, R. Thissen, A. Ruf, J. Isa, Y. Oba, T. Koga, T. Yoshimura, D. Araoka, H. Sugahara, A. Furusho, Y. Furukawa, J. Aoki, K. Kano, S.-i. M. Nomura, K. Sasaki, H. Sato, T. Yoshikawa, S. Tanaka, M. Morita, M. Onose, F.

Kabashima, K. Fujishima, T. Yamazaki, Y. Kimura, J. M. Eiler, Polycyclic aromatic hydrocarbons in samples of Ryugu formed in the interstellar medium. *Science* **382**, 1411–1416 (2023).

28. G. Wenzel, I. R. Cooke, P. B. Changala, E. A. Bergin, S. Zhang, A. M. Burkhardt, A. N. Byrne, S. B. Charnley, M. A. Cordiner, M. Duffy, Z. T. P. Fried, H. Gupta, M. S. Holdren, A. Lipnicky, R. A. Loomis, H. T. Shay, C. N. Shingledecker, M. A. Siebert, D. A. Stewart, R. H. J. Willis, C. Xue, A. J. Remijan, A. E. Wendlandt, M. C. McCarthy, B. A. McGuire, Detection of interstellar 1-cyanopyrene: A four-ring polycyclic aromatic hydrocarbon. *Science* **386**, 810–813 (2024).

29. G. Wenzel, T. H. Speak, P. B. Changala, R. H. J. Willis, A. M. Burkhardt, S. Zhang, E. A. Bergin, A. N. Byrne, S. B. Charnley, Z. T. P. Fried, H. Gupta, E. Herbst, M. S. Holdren, A. Lipnicky, R. A. Loomis, C. N. Shingledecker, C. Xue, A. J. Remijan, A. E. Wendlandt, M. C. McCarthy, I. R. Cooke, B. A. McGuire, Detections of interstellar aromatic nitriles 2-cyanopyrene and 4-cyanopyrene in TMC-1. *Nat. Astron.* **9**, 262 (2025).

30. J. Cernicharo, M. Agúndez, C. Cabezas, B. Tercero, N. Marcelino, J. R. Pardo, P. de Vicente, Pure hydrocarbon cycles in TMC-1: Discovery of ethynyl cyclopropenylidene, cyclopentadiene, and indene. *Astron. Astrophys.* **649**, L15 (2021).

31. A. M. Burkhardt, K. L. K. Lee, P. B. Changala, C. N. Shingledecker, I. R. Cooke, R. A. Loomis, H. Wei, S. B. Charnley, E. Herbst, M. C. McCarthy, B. A. McGuire, Discovery of the pure polycyclic aromatic hydrocarbon indene (c-C_9H_8) with GOTHAM observations of TMC-1. *Astrophys. J. Lett.* **913**, L18 (2021).

32. J. Cernicharo, C. Cabezas, R. Fuentetaja, M. Agúndez, B. Tercero, J. Janeiro, M. Juanes, R. I. Kaiser, Y. Endo, A. L. Steber, D. Pérez, C. Pérez, A. Lesarri, N. Marcelino, P. de Vicente, Discovery of two cyano derivatives of acenaphthylene ($C_{12}H_8$) in TMC-1 with the QUIJOTE line survey. *Astron. Astrophys.* **690**, L13 (2024).

33. N. Balucani, O. Asvany, A. H. H. Chang, S. H. Lin, Y. T. Lee, R. I. Kaiser, H. F. Bettinger, P. V. R. Schleyer, H. F. Schaefer III, Crossed beam reaction of cyano radicals with hydrocarbon molecules. I. Chemical dynamics of cyanobenzene (C_6H_5CN; X^1A_1) and perdeutero

cyanobenzene (C_6D_5CN; X^1A_1) formation from reaction of $CN(X^2\Sigma^+)$ with benzene $C_6H_6(X^1A_{1g})$, and d_6-benzene $C_6D_6(X^1A_{1g})$. *J. Chem. Phys.* **111**, 7457–7471 (1999).

34. N. Balucani, O. Asvany, L. C. L. Huang, Y. T. Lee, R. I. Kaiser, Y. Osamura, H. F. Bettinger, Formation of nitriles in the interstellar medium via reactions of cyano radicals, $CN(X^2\Sigma^+)$, with unsaturated hydrocarbons. *Astrophys. J.* **545**, 892–906 (2000).

35. Z. Yang, I. A. Medvedkov, S. J. Goettl, A. A. Nikolayev, A. M. Mebel, X. Li, R. I. Kaiser, Low-temperature gas-phase formation of cyclopentadiene and its role in the formation of aromatics in the interstellar medium. *Proc. Natl. Acad. Sci. U.S.A.* **121**, e2409933121 (2024).

36. E. R. Micelotta, A. P. Jones, A. G. G. M. Tielens, Polycyclic aromatic hydrocarbon processing in interstellar shocks. *Astron. Astrophys.* **510**, A36 (2010).

37. E. R. Micelotta, A. P. Jones, A. G. G. M. Tielens, Polycyclic aromatic hydrocarbon processing in a hot gas. *Astron. Astrophys.* **510**, A37 (2010).

38. E. R. Micelotta, A. P. Jones, A. G. G. M. Tielens, Polycyclic aromatic hydrocarbon processing by cosmic rays. *Astron. Astrophys.* **526**, A52 (2011).

39. E. Reizer, B. Viskolcz, B. Fiser, Formation and growth mechanisms of polycyclic aromatic hydrocarbons: A mini-review. *Chemosphere* **291**, 132793 (2022).

40. M. Frenklach, A. W. Jasper, A. M. Mebel, Phenalenyl growth reactions and implications for prenucleation chemistry of aromatics in flames. *Phys. Chem. Chem. Phys.* **26**, 13034–13048 (2024).

41. P. M. Mayer, V. Blanchet, C. Joblin, Threshold photoelectron study of naphthalene, anthracene, pyrene, 1,2-dihydronaphthalene, and 9,10-dihydroanthracene. *J. Chem. Phys.* **134**, 244312 (2011).

42. G. Rouillé, S. A. Krasnokutski, D. Fulvio, C. Jäger, T. Henning, G. A. Garcia, X. F. Tang, L. Nahon, Dissociative photoionization of polycyclic aromatic hydrocarbon molecules carrying an ethynyl group. *Astrophys. J.* **810**, 114 (2015).

43. Y. Li, J. Yang, Z. Cheng, Photoionization Cross Section Database, Version 2.0 (National Synchrotron Radiation Laboratory, 2017); http://flame.nsrl.ustc.edu.cn/database/data.php.

44. T. Sattasathuchana, J. S. Siegel, K. K. Baldridge, Generalized analytic approach for determination of multidimensional Franck–Condon factors: Simulated photoelectron spectra of polynuclear aromatic hydrocarbons. *J. Chem. Theory Comput.* **16**, 4521–4532 (2020).

45. Y. Tian, K. Uchida, H. Kurata, Y. Hirao, T. Nishiuchi, T. Kubo, Design and synthesis of new stable fluorenyl-based radicals. *J. Am. Chem. Soc.* **136**, 12784–12793 (2014).

46. L. Zhao, R. I. Kaiser, B. Xu, U. Ablikim, M. Ahmed, M. M. Evseev, E. K. Bashkirov, V. N. Azyazov, A. M. Mebel, Low-temperature formation of polycyclic aromatic hydrocarbons in Titan's atmosphere. *Nat. Astron.* **2**, 973–979 (2018).

47. M. Lecasble, L. Remusat, J.-C. Viennet, B. Laurent, S. Bernard, Polycyclic aromatic hydrocarbons in carbonaceous chondrites can be used as tracers of both pre-accretion and secondary processes. *Geochim. Cosmochim. Acta* **335**, 243–255 (2022).

48. H. Feuchtgruber, F. P. Helmich, E. F. van Dishoeck, C. M. Wright, Detection of interstellar CH_3. *Astrophys. J.* **535**, L111 (2000).

49. H. Jin, L. Xing, J. Hao, J. Yang, Y. Zhang, C. Cao, Y. Pan, A. Farooq, A chemical kinetic modeling study of indene pyrolysis. *Combust. Flame* **206**, 1–20 (2019).

50. A. L. Betz, Ethylene in IRC +10216. *Astrophys. J.* **244**, L103 (1981).

51. C. F. Melius, M. E. Colvin, N. M. Marinov, W. J. Pit, S. M. Senkan, Reaction mechanisms in aromatic hydrocarbon formation involving the C_5H_5 cyclopentadienyl moiety. *Symp. (Int.) Combust.* **26**, 685 (1996).

52. A. W. Jasper, N. Hansen, Hydrogen-assisted isomerizations of fulvene to benzene and of larger cyclic aromatic hydrocarbons. *Proc. Combust. Inst.* **34**, 279–287 (2013).

53. C. Cavallotti, D. Polino, On the kinetics of the C_5H_5+C_5H_5 reaction. *Proc. Combust. Inst.* **34**, 557–564 (2013).

54. C. S. McEnally, L. D. Pfefferle, An experimental study in non-premixed flames of hydrocarbon growth processes that involve five-membered carbon rings. *Combust. Sci. Technol.* **131**, 323–344 (1998).

55. R. P. Lindstedt, K. A. Rizos, The formation and oxidation of aromatics in cyclopentene and methyl-cyclopentadiene mixtures. *Proc. Combust. Inst.* **29**, 2291–2298 (2002).

56. J. Filley, J. T. McKinnon, Dimerization of cyclopentadienyl radical to produce naphthalene. *Combust. Flame* **124**, 721–723 (2001).

57. L. Zhao, R. Kaiser, W. Lu, B. Xu, M. Ahmed, A. N. Morozov, A. M. Mebel, A. H. Howlader, S. F. Wnuk, Molecular mass growth through ring expansion in polycyclic aromatic hydrocarbons via radical–radical reactions. *Nat. Commun.* **10**, 3689 (2019).

58. R. I. Kaiser, L. Zhao, W. Lu, M. Ahmed, M. V. Zagidullin, V. N. Azyazov, A. M. Mebel, Formation of benzene and naphthalene through cyclopentadienyl-mediated radical–radical reactions. *J. Phys. Chem. Lett.* **13**, 208–213 (2022).

59. J. W. Martin, K. Bowal, A. Menon, R. I. Slavchov, J. Akroyd, S. Mosbach, M. Kraft, Polar curved polycyclic aromatic hydrocarbons in soot formation. *Proc. Combust. Inst.* **37**, 1117–1123 (2019).

60. A. Bodi, M. Johnson, T. Gerber, Z. Gengeliczki, B. Sztáray, T. Baer, Imaging photoelectron photoion coincidence spectroscopy with velocity focusing electron optics. *Rev. Sci. Instrum.* **80**, 034101 (2009).

61. M. Johnson, A. Bodi, L. Schulz, T. Gerber, Vacuum ultraviolet beamline at the Swiss Light Source for chemical dynamics studies. *Nucl. Instr. Meth. Phys. Res. Sect. A* **610**, 597–603 (2009).

62. J. Bouwman, A. Bodi, P. Hemberger, Nitrogen matters: The difference between PANH and PAH formation. *Phys. Chem. Chem. Phys.* **20**, 29910–29917 (2018).

63. P. Hemberger, J. A. van Bokhoven, J. Pérez-Ramírez, A. Bodi, New analytical tools for advanced mechanistic studies in catalysis: Photoionization and photoelectron photoion coincidence spectroscopy. *Cat. Sci. Technol.* **10**, 1975–1990 (2020).

64. E. Mendez-Vega, W. Sander, P. Hemberger, Isomer-selective threshold photoelectron spectra of phenylnitrene and its thermal rearrangement products. *J. Phys. Chem. A* **124**, 3836–3843 (2020).

65. S. Grimm, S.-J. Baik, P. Hemberger, A. Bodi, A. M. Kempf, T. Kasper, B. Atakan, Gas-phase aluminium acetylacetonate decomposition: revision of the current mechanism by VUV synchrotron radiation. *Phys. Chem. Chem. Phys.* **23**, 15059–15075 (2021).

66. F. Qi, Combustion chemistry probed by synchrotron VUV photoionization mass spectrometry. *Proc. Combust. Inst.* **34**, 33–63 (2013).

67. T. A. Cool, A. McIlroy, F. Qi, P. R. Westmoreland, L. Poisson, D. S. Peterka, M. Ahmed, Photoionization mass spectrometer for studies of flame chemistry with a synchrotron light source. *Rev. Sci. Instrum.* **76**, 094102 (2005).

68. B. Sztáray, T. Baer, Suppression of hot electrons in threshold photoelectron photoion coincidence spectroscopy using velocity focusing optics. *Rev. Sci. Instrum.* **74**, 3763–3768 (2003).

69. P. Hemberger, X. Wu, Z. Pan, A. Bodi, Continuous pyrolysis microreactors: Hot sources with little cooling? New insights utilizing cation velocity map imaging and threshold photoelectron spectroscopy. *J. Phys. Chem. A* **126**, 2196–2210 (2022).

70. A. G. Baboul, L. A. Curtiss, P. C. Redfern, K. Raghavachari, Gaussian-3 theory using density functional geometries and zero-point energies. *J. Chem. Phys.* **110**, 7650–7657 (1999).

71. L. A. Curtiss, K. Raghavachari, P. C. Redfern, A. G. Baboul, J. A. Pople, Gaussian-3 theory using coupled cluster energies. *Chem. Phys. Lett.* **314**, 101–107 (1999).

72. L. A. Curtiss, K. Raghavachari, P. C. Redfern, V. Rassolov, J. A. Pople, Gaussian-3 (G3) theory for molecules containing first and second-row atoms. *J. Chem. Phys.* **109**, 7764–7776 (1998).

73. J.-D. Chai, M. Head-Gordon, Long-range corrected hybrid density functionals with damped atom–atom dispersion corrections. *Phys. Chem. Chem. Phys.* **10**, 6615–6620 (2008).

74. R. J. Bartlett, G. D. Purvis, Many-body perturbation theory, coupled-pair many-electron theory, and the importance of quadruple excitations for the correlation problem. *Int. J. Quantum Chem.* **14**, 561–581 (1978).

75. J. A. Pople, M. Head-Gordon, K. Raghavachari, Quadratic configuration interaction. A general technique for determining electron correlation energies. *J. Chem. Phys.* **87**, 5968–5975 (1987).

76. R. Krishnan, J. S. Binkley, R. Seeger, J. A. Pople, Self-consistent molecular orbital methods. XX. A basis set for correlated wave functions. *J. Chem. Phys.* **72**, 650–654 (1980).

77. M. J. Frisch, M. Head-Gordon, J. A. Pople, A direct MP2 gradient method. *Chem. Phys. Lett.* **166**, 275–280 (1990).

78. T. J. Lee, J. E. Rice, G. E. Scuseria, H. F. Schaefer, Theoretical investigations of molecules composed only of fluorine, oxygen and nitrogen: Determination of the equilibrium structures of FOOF, $(NO)_2$ and FNNF and the transition state structure for FNNF *cis-trans* isomerization. *Theor. Chim. Acta* **75**, 81–98 (1989).

79. T. J. Lee, Comparison of the T_1 and D_1 diagnostics for electronic structure theory: A new definition for the open-shell D_1 diagnostic. *Chem. Phys. Lett.* **372**, 362–367 (2003).

80. M. J. Frisch, G. W. Trucks, H. B. Schlegel, G. E. Scuseria, M. A. Robb, J. R. Cheeseman, G. Scalmani, V. Barone, B. Mennucci, G. A. Petersson, H. Nakatsuji, M. Caricato, X. Li, H. P. Hratchian, A. F. Izmaylov, J. Bloino, G. Zheng, J. L. Sonnenberg, M. Hada, M. Ehara, K. Toyota, R. Fukuda, J. Hasegawa, M. Ishida, T. Nakajima, Y. Honda, O. Kitao, H. Nakai, T. Vreven, J. Montgomery, J A, J. E. Peralta, F. Ogliaro, M. Bearpark, J. J. Heyd, E. Brothers, K. N. Kudin, V. N. Staroverov, R. Kobayashi, J. Normand, K. Raghavachari, A. Rendell, J. C. Burant, S. S. Iyengar, J. Tomasi, M. Cossi, N. Rega, J. M. Millam, M. Klene, J. E. Knox, J. B. Cross, V. Bakken, C. Adamo, J. Jaramillo, R. Gomperts, R. E. Stratmann, O. Yazyev, A. J. Austin, R. Cammi, C. Pomelli, J. W. Ochterski, R. L. Martin, K. Morokuma, V. G. Zakrzewski, G. A. Voth, P. Salvador, J. J. Dannenberg, S. Dapprich, A. D. Daniels, Ö. Farkas, J. B. Foresman, J. V. Ortiz, J. Cioslowski, D. J. Fox, *Gaussian 09, Revision A.02* (Gaussian Inc., 2009); http://www.gaussian.com.

81. H. J. Werner, P. J. Knowles, G. Knizia, F. R. Manby, M. Schütz, P. Celani, W. Györffy, D. Kats, T. Korona, R. Lindh, A. Mitrushenkov, G. Rauhut, K. R. Shamasundar, T. B. Adler, R. D. Amos, A. Bernhardsson, A. Berning, D. L. Cooper, J. O. Deegan, A. J. Dobbyn, F. Eckert, E. Goll, C. Hampel, A. Hesselmann, G. Hetzer, T. Hrenar, G. Jansen, C. Köppl, Y. Liu, A. W. Lloyd, R. A. Mata, A. J. May, S. J. McNicholas, W. Meyer, M. E. Mura, A. Nicklass, D. P. O'Neill, P. Palmieri, D. Peng, K. Pflüger, R. Pitzer, M. Reiher, T. Shiozaki, H. Stoll, A. J. Stone, R. Tarroni, T. Thorsteinsson, M. Wang, *MOLPRO, a Package of Ab Initio Programs, Version 2015.2* (University of Cardiff, 2015); http://www.molpro.net.

82. H.-J. Werner, P. J. Knowles, G. Knizia, F. R. Manby, M. Schütz, Molpro: A general-purpose quantum chemistry program package. *WIREs Comput. Mol. Sci.* **2**, 242–253 (2012).

83. S. Kim, J. Chen, T. Cheng, A. Gindulyte, J. He, S. He, Q. Li, B. A. Shoemaker, P. A. Thiessen, B. Yu, L. Zaslavsky, J. Zhang, E. E. Bolton, PubChem 2025 update. *Nucleic Acids Res.* **53**, D1516–D1525 (2024).

84. J. A. Montgomery Jr., M. J. Frisch, J. W. Ochterski, G. A. Petersson, A complete basis set model chemistry. VII. Use of the minimum population localization method. *J. Chem. Phys.* **112**, 6532–6542 (2000).

85. M. J. Frisch, G. W. Trucks, H. B. Schlegel, G. E. Scuseria, M. A. Robb, J. R. Cheeseman, G. Scalmani, V. Barone, G. A. Petersson, H. Nakatsuji, X. Li, M. Caricato, A. V. Marenich, J. Bloino, B. G. Janesko, R. Gomperts, B. Mennucci, H. P. Hratchian, J. V. Ortiz, A. F. Izmaylov, J. L. Sonnenberg, Williams, Williams, F. Ding, F. Lipparini, F. Egidi, J. Goings, B. Peng, A. Petrone, T. Henderson, D. Ranasinghe, V. G. Zakrzewski, J. Gao, N. Rega, G. Zheng, W. Liang, M. Hada, M. Ehara, K. Toyota, R. Fukuda, J. Hasegawa, M. Ishida, T. Nakajima, Y. Honda, O. Kitao, H. Nakai, T. Vreven, K. Throssell, J. A. Montgomery Jr, J. E. Peralta, F. Ogliaro, M. J. Bearpark, J. J. Heyd, E. N. Brothers, K. N. Kudin, V. N. Staroverov, T. A. Keith, R. Kobayashi, J. Normand, K. Raghavachari, A. P. Rendell, J. C. Burant, S. S. Iyengar, J. Tomasi, M. Cossi, J. M. Millam, M. Klene, C. Adamo, R. Cammi, J. W. Ochterski, R. L. Martin, K. Morokuma, O. Farkas, J. B. Foresman, D. J. Fox, *Gaussian 16, Revision C.01* (Gaussian Inc., 2016); http://www.gaussian.com.

86. S. Gozem, A. I. Krylov, The ezSpectra suite: An easy-to-use toolkit for spectroscopy modeling. *WIREs Comput. Mol. Sci.* **12**, e1546 (2022).

87. Y. Georgievskii, J. A. Miller, M. P. Burke, S. J. Klippenstein, Reformulation and solution of the master equation for multiple-well chemical reactions. *J. Phys. Chem. A* **117**, 12146–12154 (2013).

88. S. J. Klippenstein, J. I. Cline, Classical phase space theory for product state distributions with application to the *v–j* vector correlation. *J. Chem. Phys.* **103**, 5451–5460 (1995).

89. Y. Georgievskii, S. J. Klippenstein, Master Equation System Solver [MESS], 2016.3.23 (2015); https://tcg.cse.anl.gov/papr.

90. J. P. Maier, D. W. Turner, Steric inhibition of resonance studied by molecular photoelectron spectroscopy. Part 1—Biphenyls. *Faraday Discuss. Chem. Soc.* **54**, 149–167 (1972).

91. L. Crisci, S. Di Grande, C. Cavallotti, V. Barone, Toward an accurate black-box tool for the kinetics of gas-phase reactions involving barrier-less elementary steps. *J. Chem. Theory Comput.* **19**, 7626–7639 (2023).

92. J. F. Alarcon, A. N. Morozov, A. M. Mebel, A. Della Libera, L. Pratali Maffei, C. Cavallotti, Mechanism and kinetics of the oxidation of propargyl radical by atomic oxygen. *Proc. Combust. Inst.* **40**, 105372 (2024).